ACS central science

Research Article

http://pubs.acs.org/journal/acscii

Superior Charge Storage and Power Density of a Conducting Polymer-Modified Covalent Organic Framework

Catherine R. Mulzer,[†] Luxi Shen,[†] Ryan P. Bisbey,[†,‡] James R. McKone,[†] Na Zhang,[†] Héctor D. Abruña,*[,†] and William R. Dichtel*[,†,‡]

[†]Department of Chemistry and Chemical Biology, Baker Laboratory, Cornell University, Ithaca, New York 14853-1301, United States

[‡]Department of Chemistry, Northwestern University, Evanston, Illinois 60208, United States

Supporting Information

ABSTRACT: The low conductivity of two-dimensional covalent organic frameworks (2D COFs), and most related coordination polymers, limits their applicability in optoelectronic and electrical energy storage (EES) devices. Although some networks exhibit promising conductivity, these examples generally lack structural versatility, one of the most attractive features of framework materials design. Here we enhance the electrical conductivity of a redox-active 2D COF film by electropolymerizing 3,4-ethylenedioxythiophene (EDOT) within its pores. The resulting poly(3,4-ethylenedioxythiophene) (PEDOT)-infiltrated COF films exhibit dramatically improved electrochemical responses, including quantitative access to their redox-active groups, even for 1 μm-thick COF films that otherwise provide poor electrochemical performance. PEDOT-modified COF films can accommodate high charging rates (10−1600 C) without compromising performance and exhibit both a 10-fold higher current response relative to unmodified films and stable capacitances for at least 10 000 cycles. This work represents the first time that electroactive COFs or crystalline framework materials have shown volumetric energy and power densities comparable with other porous carbon-based electrodes, thereby demonstrating the promise of redox-active COFs for EES devices.

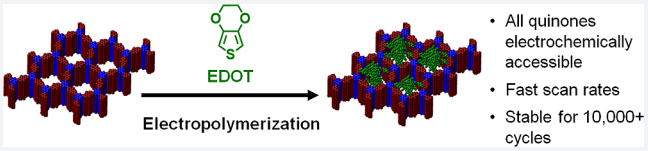

INTRODUCTION

Pseudocapacitors can combine the high energy density of batteries and superior power densities of double-layer capacitors[1−3] by storing electricity through both the nonfaradaic formation of an electrochemical double layer (EDL) and reversible faradaic redox processes of surface bound/immobilized species.[4−7] Nanoporous electrodes, often carbon-based materials, feature high specific surface areas that maximize electrochemical double-layer formation.[8−10] Although redox-active groups have been covalently bonded or adsorbed to these electrodes,[11−13] their performance is often compromised by charge transfer and counterion transport limitations. In addition, their poorly defined structures complicate characterization and rational improvement.[14,15] Two-dimensional covalent organic frameworks (2D COFs) address these limitations by predictably and deliberately organizing redox-active groups into insoluble, high-surface area polymer networks with uniform micropores.[16−19] However, the modest conductivity of existing 2D COFs has limited devices to thin films of the active material (50−250 nm) grown on Au[20] or carbon nanotube[21] electrodes that only operate at slow charge/discharge rates, limiting high power performance. Here we address this challenge by electropolymerizing EDOT into the pores of redox-active 2D COF films. The resulting poly(3,4-ethylenedioxythiophene) (PEDOT)-modified COF films (Figure 1) exhibit quantitative electrochemical accessibility of their redox-active groups and enable the use of at least 1 μm thick films that can sustain fast charging rates (up to 1600 C) without compromising performance. This improved performance relative to as-synthesized COF films corresponds to a 30-fold increase in volumetric energy density and a 12-fold increase in volumetric power density, two important metrics for evaluating thin film capacitors.[22]

The electropolymerization of PEDOT within a nanoporous COF template represents a means to organize the conductive polymer at the nanometer length scale, which is an increasingly important capability for electrochromic, drug delivery, electrocatalytic, and EES devices, among other applications.[23−27] Templated electropolymerizations form conducting polymers, such as polypyrrole, polythiophene, or polyaniline, as nanowire arrays,[28] which respond rapidly in electrochemical devices largely because of short counterion diffusion lengths.[26−28] In these examples, the porous templates are removed. Here we observe a synergistic effect in which the pore-confined PEDOT effectively wires the redox-active groups of the COF to the electrode, enabling the use of thicker films and dramatically faster charging rates.

RESULTS AND DISCUSSION

PEDOT was electropolymerized within a 2,6-diaminoanthraquinone-2,4,6-triformylphloroglucinol (DAAQ-TFP) thin-film working electrode via cyclic voltammetry in a 100 mM CH_3CN solution of EDOT containing 100 mM $(n\text{-Bu})_4NClO_4$ (TBAP)

Received: August 6, 2016
Published: August 24, 2016

DOI: 10.1021/acscentsci.6b00220
ACS Cent. Sci. 2016, 2, 667−673

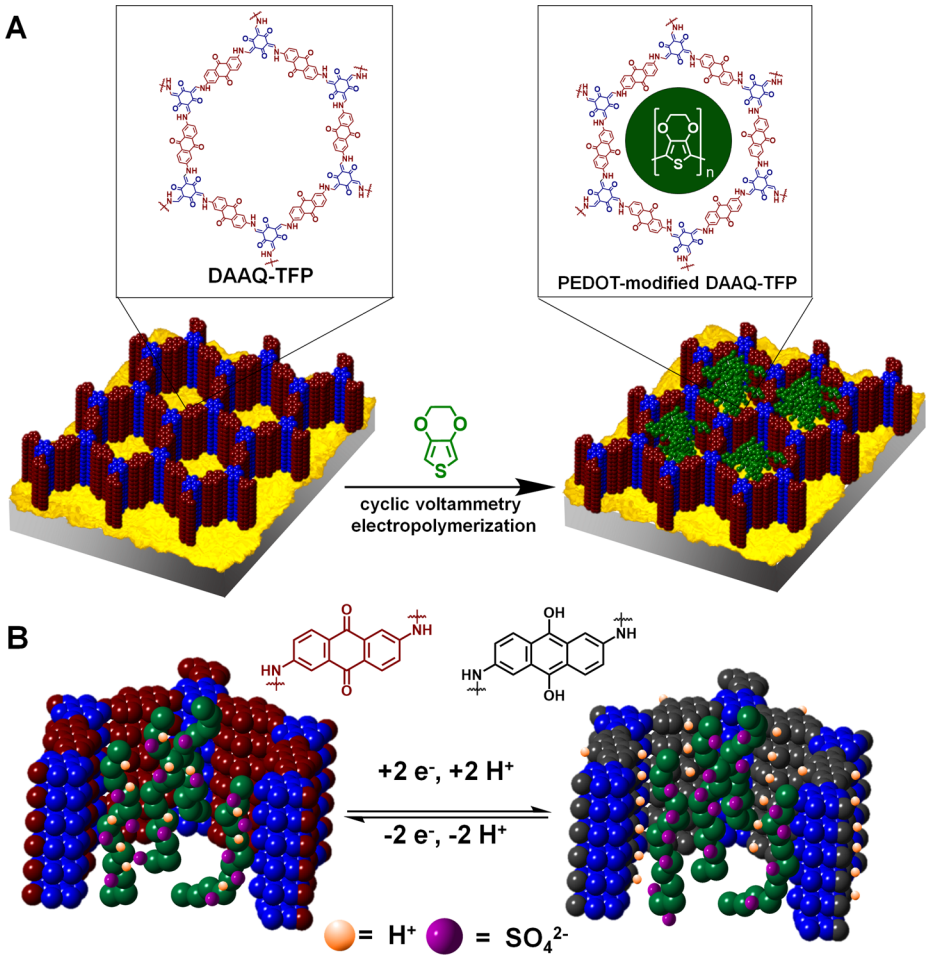

Figure 1. Incorporation of PEDOT within a DAAQ-TFP COF film. (A) Depiction of modification of DAAQ–TFP films by electropolymerization of 3,4-ethylenedioxythiophene (EDOT). Schematic depicts what may occur within one COF crystallite. (B) Schematic of the cross-section of a pore following the oxidation and reduction of the DAAQ moieties.

as the supporting electrolyte. DAAQ–TFP thin films were prepared by adding a DMF solution of TFP over 1 h to a DMF solution of DAAQ containing a gold substrate.[20] Similar to our previous report, we isolate polycrystalline thin films whose thickness was controlled by varying the initial monomer concentration. For example, an initial DAAQ concentration ($[DAAQ]_0$) of 22 mM yielded DAAQ–TFP thin films of 810 ± 224 nm thickness, as determined by atomic force microscopy (AFM, Figures S1–S4). The chemical composition of the COF films was assessed using Fourier transform infrared (FT-IR) and X-ray photoelectron spectroscopy (XPS). Their morphology was characterized by scanning electron microscopy (SEM, Figures S5 and S6), and their crystallinity was measured using grazing incidence X-ray diffraction (GIXD, Figures S7–S9). These measurements are consistent with those of thinner films reported previously[20,29,30] and indicate the formation of crystalline DAAQ-TFP films whose layered crystallites are preferentially oriented parallel to the substrate (Figures S4–S8). The amount of PEDOT incorporated into the 2D COF film was characterized by two independent measurements: the current passed during each electropolymerization cycle (−0.5–1.0 V vs $Ag/AgClO_4$, 20 mV s^{-1} scan rate) and the mass deposited onto a COF-modified electrode, as detected using an electrochemical quartz crystal microbalance (EQCM, Figure 2A,B). In the first cycle, 15 μg of PEDOT and electrolyte were deposited per cm^2 of the working electrode's geometric area, which increased to 30 $\mu g\ cm^{-2}$ for the second and subsequent cycles. Because of viscoelastic losses over the course of the experiment, the Sauerbrey equation overestimates these masses (see Supporting Information for further discussion, Figures S10 and S11). During the reductive sweep of each electropolymerization cycle, there is a mass loss corresponding to removal of perchlorate counterions (dedoping) from the film to maintain electroneutrality.[31] The voltammetric response exhibited an increase in current with each scan, which is characteristic of PEDOT electropolymerization (Figure 2B), and the redox processes occurred at voltages consistent with those expected for EDOT oxidation.[32–35] FT-IR spectra of the films, acquired before and after the electropolymerization, suggest the formation of PEDOT and that the DAAQ–TFP's chemical linkages are retained. After two electropolymerization cycles, the FT-IR spectrum of the film was almost identical to that of the as-synthesized DAAQ–TFP film. Both spectra exhibited peaks at 1250 cm^{-1}, 1560 cm^{-1}, and 1615 cm^{-1}, corresponding to intact β-ketoenamine C–N, C=C, and C=O stretches, respectively. After nine electropolymerization cycles, spectral features resembling bulk PEDOT emerge, though absorbances associated with the β-ketoenamine remain, albeit with lower relative intensities (Figure 2C). Grazing incidence X-ray diffraction (GIXD) experiments, performed at the Cornell High Energy Synchrotron Source (CHESS), indicate that the as-synthesized DAAQ–TFP films are

DOI: 10.1021/acscentsci.6b00220
ACS Cent. Sci. 2016, 2, 667–673

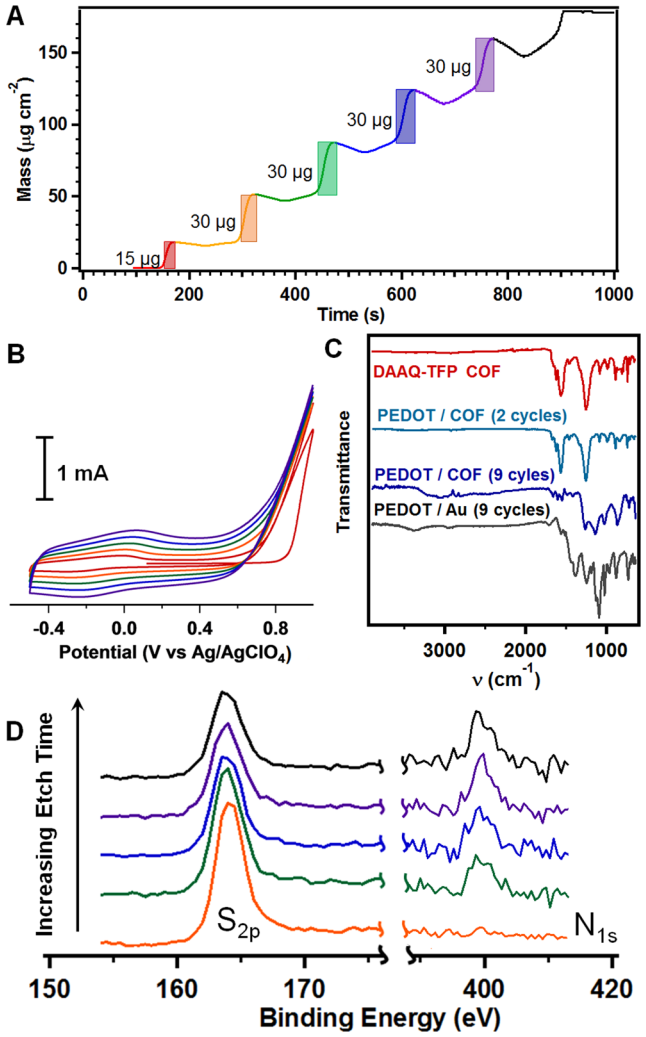

Figure 2. Modification of a DAAQ–TFP film via electropolymerization of PEDOT. (A) Electrochemical QCM data showing separate polymerization cycles (red, first; orange, second; green, third; blue, fourth; purple, fifth) showing a consistent mass increase of 30 μg cm^{-2} per cycle except for the first cycle (15 μg cm^{-2}). (B) Cyclic voltammograms at 20 mV s^{-1} during the EDOT electropolymerization. Each cycle is colored to correspond with panel A (red, first; orange, second; green, third; blue, fourth; purple, fifth). (C) FTIR spectra of an as-synthesized DAAQ–TFP film (red), the film after two electropolymerization cycles (light blue), a film after nine electropolymerization cycles (blue), and PEDOT (black). (D) XPS depth profile (Ar ion beam etch) of the N_{1s} and S_{2p} regions (orange, first step; green, second step; blue, third step; purple, fourth step; black, fifth step). The N_{1s} profiles are scaled 3-fold in intensity for visual clarity.

crystalline, with a peak at 0.23 Å^{-1} that corresponds to the (100) reflection of the hexagonal lattice. This peak was also observed in films that were subjected to two electropolymerization cycles, indicating that the periodicity of the DAAQ–TFP thin film is retained under the electropolymerization conditions. After nine cycles, this peak is not observed, which is not unexpected after depositing amorphous PEDOT within the ordered DAAQ–TFP COF (Figures S7–S9). For example, Russell et al. reported that the scattered intensity diminishes when a porous host is filled with a polymer of similar electron density.[36] The surface area of the films before and after PEDOT polymerization, as measured using Kr adsorption (Figure S12), was also consistent with the deposition of the polymer into the pores of the DAAQ–TFP COF. Unmodified DAAQ–TFP films exhibited Brunauer–Emmett–Teller surface areas (S_{BET}) of 73 cm^2 per cm^2 of substrate. This value decreased to 40 cm^2 per cm^{-2} after two electropolymerization cycles, and films subjected to nine electropolymerization cycles appeared nearly nonporous (S_{BET} = 6 cm^2 cm^{-2}). An X-ray photoelectron spectroscopy (XPS) depth profile of the elemental composition of a PEDOT-modified DAAQ-TFP film subjected to nine electropolymerization cycles further indicates the presence of PEDOT throughout the 2D COF film. XPS spectra were recorded after a series of exposures to an Ar ion beam that etches both the PEDOT and the COF. Prior to etching, an intense S_{2p} signal (164.9 eV) is observed, along with no signal above baseline in the N_{1s} region (399.2 eV), which we attribute to a thin PEDOT overgrowth layer on top of the COF film. After the first etching cycle, N_{1s} and S_{2p} signals are both observed in five subsequent consecutive spectra (Figure 2D), and, after prolonged etching, the entire film is removed. These combined observations indicate that PEDOT electropolymerization occurs in the pores of the COF film and that the conductive polymer effectively infiltrates the COF structure.

The PEDOT-modified DAAQ–TFP composite films exhibited dramatically enhanced current responses in cyclic voltammetry (CV) experiments when compared to an unmodified DAAQ–TFP film (0.5 M H_2SO_4, 20 mV s^{-1} scan rate, Figure 3A). While both CVs exhibit reversible electrochemistry consistent with electron transfer between the anthraquinones and the working electrode, the PEDOT-modified DAAQ–TFP films exhibited more than an order of magnitude increased current. These responses correspond to a faradaic charge storage of only 0.230 mC, corresponding to only 3% of the available anthraquinones for a representative unmodified, 1 μm-thick DAAQ–TFP film (see Supporting Information for a sample calculation of electrochemically addressed anthraquinones, Figure S13). This value increased to 9.3 mC after the same DAAQ–TFP sample was modified with PEDOT, corresponding to a 40-fold increase in accessible charge. In contrast to the unmodified COF films, PEDOT-modified films retain their well-defined redox responses and charge densities at scan rates up to 500 mV s^{-1} (Figure 3B). In contrast, the already small percentage of accessible anthraquinones (3%) measured at 20 mV s^{-1} decreased to less than 1% at sweep rates above 100 mV s^{-1} (Figure 3B).

Having established the dramatic enhancement in performance associated with modifying COF thin films with PEDOT, we determined the optimal electropolymerization conditions (nine cycles, 20 mV s^{-1}; see Supporting Information for details Figures S14–S16) for maximizing the charge stored and accessed at high scan rates (100–500 mV s^{-1}) while maintaining electrolyte access to the framework. While additional electropolymerization cycles increased the capacitance associated with additional PEDOT coverage, the faradaic contribution remained constant at a value corresponding to a quantitative access to the quinone sites (Figure S14). These experiments indicate that the electropolymerization of PEDOT in a redox-active COF film provides dramatically enhanced charge storage capacitance and rate. These effects most likely arise from intimately mixing PEDOT in the COF for improved conductivity of the PEDOT-modified DAAQ-TFP film, which was assessed using electrochemical impedance spectroscopy (EIS, Figures S17 and S18, Table S1). We used a two constant-

DOI: 10.1021/acscentsci.6b00220
ACS Cent. Sci. 2016, 2, 667–673

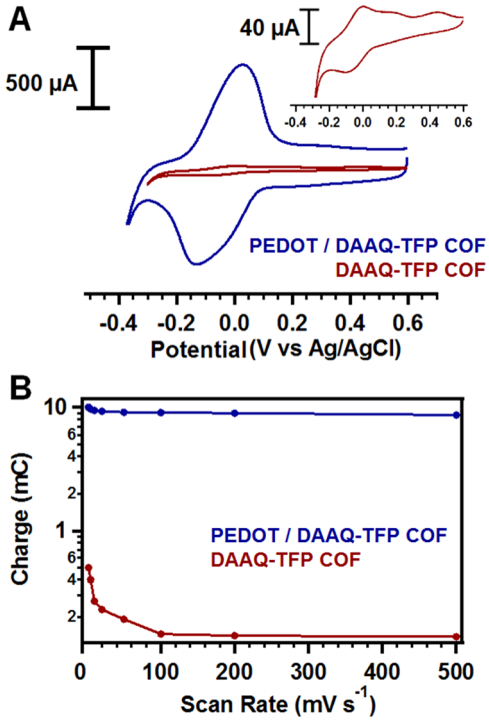

Figure 3. Electrochemical performance of a PEDOT-modified and as-synthesized DAAQ–TFP COF film. (A) CV response at 20 mV s^{-1} in 0.5 M H_2SO_4 of a PEDOT-modified DAAQ–TFP film, 1 μm-thick (blue), and the same as-synthesized DAAQ–TFP film before EDOT polymerization (red). The inset presents the cyclic voltammetric response for the unmodified film using an expanded current scale. (B) The integrated charge associated with the oxidative wave of a PEDOT-modified DAAQ–TFP COF film (blue) and unmodified DAAQ–TFP COF film (red) recorded over various scan rates indicate that the PEDOT-modified films store more charge and tolerate faster scan rates than the unmodified films.

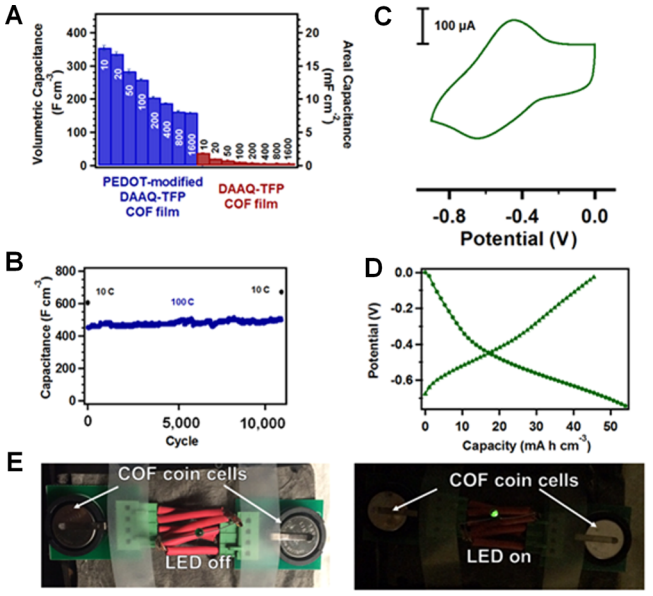

Figure 4. Charge storage performance and device integration of a PEDOT-modified DAAQ–TFP film. (A) Average capacitances calculated from 10 cycles of galvanostatic charge–discharge experiments at various C rates (error bars show ±1 standard deviation). (B) Extended cycling of a PEDOT-modified DAAQ–TFP film showing stability over 10 000 cycles. First three cycles are at a rate of 10 C, then over 10 000 cycles at a rate of 100 C, followed by another three cycles at 10 C showing no loss in capacitance over the cycles. (C) CV in a two-electrode device configuration, in which the counter is a high-surface area carbon electrode. (D) A potential/capacity plot obtained in a two-electrode experiment exhibits well-defined voltage plateaus at the formal potential of the DAAQ moieties. (E) A PEDOT-modified DAAQ–TFP COF working device powering a green LED.

phase-element (2CPE) model, in series with the solution resistance (R_s), to model the EIS data. The R_s was more than an order of magnitude lower for the PEDOT-modified DAAQ–TFP film (R_s = 20 Ω) than the unmodified DAAQ–TFP (R_s = 430 Ω), demonstrating an increased conductivity when PEDOT is incorporated into the films.

Given the superior electrochemical performance of the PEDOT-modified DAAQ-TFP films, their capacitance was evaluated through galvanostatic charge–discharge experiments performed at various charging rates (C), where nC corresponds to charging or discharging of the film over $1/n$ hours (Figures S19–S24, Table S2). PEDOT-modified DAAQ–TFP electrodes consistently showed higher capacitances than those lacking PEDOT and retained more than 80% of their capacitance when charged or discharged at 10 and 100 C, corresponding to charge times of 360 and 36 s, respectively. The PEDOT-modified DAAQ–TFP film even retains 50% of its maximum capacitance (350 F cm^{-3}) at the extremely high charging rate of 1600 C, corresponding to a charging time of only 2.25 s (Figure 4A). In contrast, the unmodified DAAQ–TFP films show only moderate capacitances at 10 C (20 F cm^{-3}), which decreased further at higher charge/discharge rates. The PEDOT-modified DAAQ–TFP films also showed outstanding stability over 10 000 charge–discharge cycles (Figure 4B). The capacitance of the film was measured at 10 C for three cycles, then at 100 C for 10 000 cycles, and finally three more cycles at 10 C. No decrease in capacitance was observed under these conditions.

To further probe the stability, we conducted a potentiostatic experiment where we held the composite film at a reducing potential (−0.3 V vs Ag/AgCl) for 15 h, after which no degradation in the CV response was observed, Figure S25). We examined the possibility for slow internal electron transfer between the PEDOT in its oxidized, conducting form and the reduced anthraquinone moieties by performing a scan rate dependence experiment at slow cycling rates (0.5, 1, 5, 10, 20, 50, 100, 300, 500 mV s^{-1}). Since the integrated charge for anthraquinone reduction is greater than that of the integrated oxidative wave, we hypothesize that a portion of the reduced anthraquinone moieties transfer electrons and reduce the oxidized PEDOT (effectively a "self-discharge" mechanism). However, the Coulombic efficiency becomes quantitative at scan rates above 10 mV s^{-1}, suggesting that process is not occurring at the operational C rates and is not detrimental to the composite electrode performance (see Figure S26 and accompanying discussion).

To determine the relative contributions of the faradaic and nonfaradaic processes at both fast and slow scan rates, GCDC experiments were performed between 0.35–0.6 V vs Ag/$AgClO_4$, where the DAAQ moieties are redox-inactive, and compared them to an experiment performed over the full −0.3–0.6 V vs Ag/$AgClO_4$ range (Figure S22, Table S2). This comparison indicates that both the DAAQ moieties and the PEDOT contribute nearly equally to the capacitance at all tested charging rates, demonstrating the synergistic effect of combining the two materials. We also examined the performance of a PEDOT composite of a nonredox-active COF based

DOI: 10.1021/acscentsci.6b00220
ACS Cent. Sci. 2016, 2, 667–673

on 1,4-diaminobenzene (DAB), DAB–TFP COF,[28] which showed capacitances comparable to PEDOT contribution of the PEDOT-modified DAAQ–TFP composite (Figure S23). Furthermore, Au electrodes modified only with electropolymerized PEDOT exhibited a similar double-layer capacitance as the PEDOT/COF hybrid, but lacked the enhanced charge storage associated with the DAAQ redox couple, as determined from the lack of voltage plateau in the potential/capacity plots (Figures S20 and S21).

As described by Ruoff and co-workers, performance metrics are more appropriately evaluated using a two electrode configuration;[37] therefore, we probed the PEDOT-modified DAAQ–TFP films using a high surface area carbon counter and quasireference, where the size and mass of the carbon counter was significantly greater than that of the active film. Under these conditions (20 mV s^{-1}, 0.5 M H_2SO_4), the films exhibit reversible oxidation and reduction waves (Figure 4C) that are associated with pseudocapacitive features in a two-electrode configuration.[37] GCDC profiles exhibited well-defined voltage plateaus consistent with previous experiments (Figure 4D) and capacitances comparable to those observed in a three-electrode system at charging rates up to 800 C. At still faster charging rates, device performance was limited by the counter electrode, not the COF film (Figure S27).

As a proof-of-principle for integrating larger amounts of the COF into devices, we fabricated coin cell devices, which were characterized and used to power a light emitting diode (LED, Figure 4E). Since the quantity of the PEDOT-modified COF obtained from electropolymerization is on the order of micrograms, we turned to insoluble polycrystalline DAAQ–TFP COF powder and a $Fe(ClO_4)_3$ chemical polymerization of EDOT within the pores to afford bulk PEDOT-modified DAAQ–TFP COF (see Supporting Information for fabrication procedures, Figures S28–S32 and Table S3). The crystallinity and chemical composition of these materials were confirmed using X-ray powder diffraction and IR spectroscopy (Figures S29 and S30). A 4 mg portion of PEDOT-modified DAAQ–TFP COF powder (1:1 PEDOT/COF by mass as active electrode and activated carbon counter electrode) was integrated into coin cells. When two of these cells were connected in series, they successfully powered a green LED for 30 s (see Supplemental Video). Electrochemical performance testing of the cells show that they exhibit well-defined redox waves associated with the reduction and oxidation of the anthraquinone moieties in both the CV and GCDC responses (Figures S31 and S32) with a capacitance of 197 F g^{-1} based on the active composite electrode or 30 F g^{-1} when the mass of the active and counter electrodes are considered. Notably, these cells are not optimized, and the gravimetric capacitances are expected to increase if the minimal mass of counter electrode and PEDOT to elicit the same electrochemical performance are identified. However, they demonstrate a means to fabricate working charge storage devices from conducting polymer-modified COFs, even as methods to access thicker films continue to emerge.

CONCLUSION

Prior to this work, 2D COFs had shown promise for EES devices only when used either as few-layer sheets or very thin films (~50 nm)[20,21,38,39] because of their limited conductivity. Although some coordination polymers circumvent this issue through elegant linkage chemistries,[40] such approaches limit the scope of accessible frameworks. The facile electropolymerization of EDOT within the pores of comparably thick COF films (~1 μm) enhances the framework's conductivity to provide complete electrochemical addressability of redox-active groups within the COF, even at very high scan rates. The complete electrochemical accessibility and fast charging rates of the COF/PEDOT composites show significant improvements in volumetric energy and power densities relative to unmodified COF films, as well as outstanding stability to cycling. These findings justify follow-up efforts to access and probe even thicker COF films, further optimize the COF and conducting polymer structures, and explore other applications that will benefit from the enhanced electrical conductivity of the hybrid films. Positive developments in these directions will continue to demonstrate the promise of designed, structurally precise organic materials for EES devices.

METHODS

Synthesis of DAAQ–TFP Films. DAAQ (17 mg, 0.071 mmol) in *N*,*N*-dimethylformamide was added to a glass vial. A gold electrode (2.5 cm × 1.3 cm) was submerged in the solution, and a septum was used to seal the vial. The solution was placed on a hot plate preheated to 90 °C. Subsequently, TFP (10 mg, 0.048 mmol) was added over the course of 1 h via syringe from a 10 mg mL^{-1} solution in DMF. During the course of the addition, the reaction mixture was gently swirled. After the addition, the reaction was allowed to proceed at 90 °C for an additional 3 h. The total reaction time was 4 h (including TFP addition), and the final volume was 4.2 mL after TFP addition. After the reaction was complete, the film which covered electrode was removed, rinsed three times with DMF and twice with acetone, and then dried in air.

Electropolymerization of 3,4-Ethylenedioxythiophene (EDOT). Electropolymerization was carried out in a standard three electrode set up under an argon atmosphere with a DAAQ–TFP COF film on gold (prepared as described above) as the working electrode, a $Ag/AgClO_4$ reference electrode, and either a coiled Pt wire or high surface area carbon counter electrode. A controlled area (0.64 cm^2) surface cell was used for electrochemistry experiments. A 0.1 M solution of EDOT was prepared in 0.1 M TBAP, and nine electropolymerization cycles between −0.5 and 1.1 V vs $Ag/AgClO_4$ at 20 mV s^{-1} were carried out. After electropolymerization, the PEDOT-modified DAAQ-TFP on gold was rinsed 3× with acetonitrile and 2× with acetone before electrochemical testing.

Height Analysis of Films. AFM was used to determine film thicknesses both before and after electropolymerization of EDOT. Film heights were obtained from averaging step edges at three locations on the film (see Supporting Information for further details).

Electrochemical Testing of PEDOT-Modified DAAQ–TFP Films. After electropolymerization, the prepared films were rinsed as described above and submerged in 0.5 M H_2SO_4. For initial testing, cyclic voltammetry with scan rate dependence or galvanostatic charge/discharge experiments were performed in a three electrode configuration. Capacitances were obtained from the discharge curves by multiplying the applied current by the time of discharge and normalizing by the examined voltage window and geometric film volume. Film volumes were obtained from the electrochemical cell area and the experimentally determined film thicknesses as described above. Sample calculations can be found in the Supporting Information. Thin films were also tested in a two-electrode thin

DOI: 10.1021/acscentsci.6b00220
ACS Cent. Sci. 2016, 2, 667–673

film setup where films were countered to a high surface area carbon after shorting the reference and counter electrode together. Sample calculations for volumetric capacitance and electrochemically accessible anthraquinones can be found in the Supporting Information.

Sample calculations of volumetric capacitances can be found in the Supporting Information.

■ ASSOCIATED CONTENT

Supporting Information

The Supporting Information is available free of charge on the ACS Publications website at DOI: 10.1021/acscentsci.6b00220.

Experimental details, sample calculations, and additional electrochemical characterization (PDF)

Supplemental video (AVI)

■ AUTHOR INFORMATION

Corresponding Authors

*(H.D.A.) E-mail: hda1@cornell.edu.

*(W.R.D.) E-mail: wdichtel@northwestern.edu.

Notes

The authors declare no competing financial interest.

■ ACKNOWLEDGMENTS

This research was supported by the NSF in the form of an NSF GRFP (DGE-1144153) award to C.R.M. W.R.D. acknowledges the Camille and Henry Dreyfus Foundation for a Camille Dreyfus Teacher-Scholar Award, and the Army Research Office for a Multidisciplinary University Research Initiatives (MURI) Award under Grant Number W911NF-15-1-0447. This work was supported in part (L.S., J.R.M, N.Z., H.D.A.) by the DOE through Grant DE-FG02-87ER45298, by the Energy Materials Center at Cornell (emc^2), an Energy Frontier Research Center funded by the DOE Office of Basic Energy Sciences (DE-SC000001086) and an Innovation Economy Matching Grant from the New York State, Empire State Development Division of Science, Technology and Innovation (NYSTAR), under Contract Number C090148. J.R.M. acknowledges research support through the U.S. Department of Energy, Office of Energy Efficiency and Renewable Energy, through a SunShot postdoctoral research award. This research made use of the Cornell Center for Materials Research Facilities supported by the NSF (DMR-1120296). This work made use of the Nanobiotechnology Center shared research facilities at Cornell.

■ REFERENCES

(1) Dunn, B.; Kamath, H.; Tarascon, J.-M. Electrical Energy Storage for the Grid: A Battery of Choices. *Science* **2011**, *334*, 928−935.

(2) Tarascon, J.-M.; Armand, M. Issues and Challenges Facing Rechargeable Lithium Batteries. *Nature* **2001**, *414*, 359−367.

(3) Goodenough, J. B.; Abruña, H. D. *Basic Research Needs for Electrical Energy Storage*; Office of Basic Sciences, U.S. Department of Energy: Washington, D.C., 2007.

(4) Wang, G.; Zhang, L.; Zhang, J. A Review of Electrode Materials for Electrochemical Supercapacitors. *Chem. Soc. Rev.* **2012**, *41*, 797−828.

(5) Winter, M.; Brodd, R. J. What Are Batteries, Fuel Cells, and Supercapacitors? *Chem. Rev.* **2004**, *104*, 4245−4270.

(6) Conway, B. E. *Electrochemical Supercapacitors*; Springer US: Boston, MA, 1999.

(7) Simon, P.; Gogotsi, Y. Materials for Electrochemical Capacitors. *Nat. Mater.* **2008**, *7*, 845−854.

(8) Chmiola, J.; Yushin, G.; Gogotsi, Y.; Portet, C.; Simon, P.; Taberna, P. L. Anomalous Increase in Carbon Capacitance at Pore Sizes Less than 1 Nanometer. *Science* **2006**, *313*, 1760−1763.

(9) Zhu, Y.; Murali, S.; Stoller, M. D.; Ganesh, K. J.; Cai, W.; Ferreira, P. J.; Pirkle, A.; Wallace, R. M.; Cychosz, K. A.; Thommes, M.; et al. Carbon-Based Supercapacitors Produced by Activation of Graphene. *Science* **2011**, *332*, 1537−1541.

(10) Chmiola, J.; Largeot, C.; Taberna, P.-L.; Simon, P.; Gogotsi, Y. Monolithic Carbide-Derived Carbon Films for Micro-Supercapacitors. *Science* **2010**, *328*, 480−483.

(11) Wang, Y.; Bai, Y.; Li, X.; Feng, Y.; Zhang, H. A General Strategy Towards Encapsulation of Nanoparticles in Sandwiched Graphene Sheets and the Synergic Effect on Energy Storage. *Chem. - Eur. J.* **2013**, *19*, 3340−3347.

(12) Dai, L. Functionalization of Graphene for Efficient Energy Conversion and Storage. *Acc. Chem. Res.* **2013**, *46*, 31−42.

(13) Huang, H.; Nazar, L. F. Grafted Metal Oxide/Polymer/Carbon Nanostructures Exhibiting Fast Transport Properties. *Angew. Chem., Int. Ed.* **2001**, *40*, 3880−3884.

(14) To, J. W. F.; Chen, Z.; Yao, H.; He, J.; Kim, K.; Chou, H.-H.; Pan, L.; Wilcox, J.; Cui, Y.; Bao, Z. Ultrahigh Surface Area Three-Dimensional Porous Graphitic Carbon from Conjugated Polymeric Molecular Framework. *ACS Cent. Sci.* **2015**, *1*, 68−76.

(15) Forse, A. C.; Merlet, C.; Griffin, J. M.; Grey, C. P. New Perspectives on the Charging Mechanisms of Supercapacitors. *J. Am. Chem. Soc.* **2016**, *138*, 5731−5744.

(16) Feng, X.; Ding, X.; Jiang, D. Covalent Organic Frameworks. *Chem. Soc. Rev.* **2012**, *41*, 6010−6022.

(17) Ding, S.-Y.; Wang, W. Covalent Organic Frameworks (COFs): From Design to Applications. *Chem. Soc. Rev.* **2013**, *42*, 548−568.

(18) Colson, J. W.; Dichtel, W. R. Rationally Synthesized Two-Dimensional Polymers. *Nat. Chem.* **2013**, *5*, 453−465.

(19) Côté, A. P.; Benin, A. I.; Ockwig, N. W.; O'Keeffe, M.; Matzger, A. J.; Yaghi, O. M. Porous, Crystalline, Covalent Organic Frameworks. *Science* **2005**, *310*, 1166−1170.

(20) DeBlase, C. R.; Hernández-Burgos, K.; Silberstein, K. E.; Rodríguez-Calero, G. G.; Bisbey, R. P.; Abruña, H. D.; Dichtel, W. R. Rapid and Efficient Redox Processes within 2D Covalent Organic Framework Thin Films. *ACS Nano* **2015**, *9*, 3178−3183.

(21) Xu, F.; Jin, S.; Zhong, H.; Wu, D.; Yang, X.; Chen, X.; Wei, H.; Fu, R.; Jiang, D. Electrochemically Active, Crystalline, Mesoporous Covalent Organic Frameworks on Carbon Nanotubes for Synergistic Lithium-Ion Battery Energy Storage. *Sci. Rep.* **2015**, *5*, 8225.

(22) Gogotsi, Y.; Simon, P. True Performance Metrics in Electrochemical Energy Storage. *Science* **2011**, *334*, 917−918.

(23) Cho, S. I.; Kwon, W. J.; Choi, S.-J.; Kim, P.; Park, S.-A.; Kim, J.; Son, S. J.; Xiao, R.; Kim, S.-H.; Lee, S. B. Nanotube-Based Ultrafast Electrochromic Display. *Adv. Mater.* **2005**, *17*, 171−175.

(24) Shi, Y.; Peng, L.; Ding, Y.; Zhao, Y.; Yu, G. Nanostructured Conductive Polymers for Advanced Energy Storage. *Chem. Soc. Rev.* **2015**, *44*, 6684−6696.

(25) Wang, L.; Feng, X.; Ren, L.; Piao, Q.; Zhong, J.; Wang, Y.; Li, H.; Chen, Y.; Wang, B. Flexible Solid-State Supercapacitor Based on a Metal−Organic Framework Interwoven by Electrochemically-Deposited PANI. *J. Am. Chem. Soc.* **2015**, *137*, 4920−4923.

(26) Boota, M.; Paranthaman, M. P.; Naskar, A. K.; Li, Y.; Akato, K.; Gogotsi, Y. Waste Tire Derived Carbon−Polymer Composite Paper as Pseudocapacitive Electrode with Long Cycle Life. *ChemSusChem* **2015**, *8*, 3576−3581.

(27) MacLean, M. W. A.; Kitao, T.; Suga, T.; Mizuno, M.; Seki, S.; Uemura, T.; Kitagawa, S. Unraveling Inter- and Intrachain Electronics in Polythiophene Assemblies Mediated by Coordination Nanospaces. *Angew. Chem., Int. Ed.* **2016**, *55*, 708−713.

(28) Cai, Z.; Lei, J.; Liang, W.; Menon, V.; Martin, C. R. Molecular and Supermolecular Origins of Enhanced Electric Conductivity in Template-Synthesized Polyheterocyclic Fibrils. 1. Supermolecular Effects. *Chem. Mater.* **1991**, *3*, 960−967.

(29) Kandambeth, S.; Mallick, A.; Lukose, B.; Mane, M. V.; Heine, T.; Banerjee, R. Construction of Crystalline 2D Covalent Organic

Frameworks with Remarkable Chemical (Acid/base) Stability via a Combined Reversible and Irreversible Route. *J. Am. Chem. Soc.* **2012**, *134*, 19524−19527.
(30) DeBlase, C. R.; Silberstein, K. E.; Truong, T.-T.; Abruña, H. D.; Dichtel, W. R. β-Ketoenamine-Linked Covalent Organic Frameworks Capable of Pseudocapacitive Energy Storage. *J. Am. Chem. Soc.* **2013**, *135*, 16821−16824.
(31) Naoi, K.; Lien, M. M.; Smyrl, W. H. Quartz Crystal Microbalance Analysis. *J. Electroanal. Chem. Interfacial Electrochem.* **1989**, *272*, 273−275.
(32) Oyama, N.; Kiya, Y.; Hatozaki, O.; Morioka, S.; Abruña, H. D. Dramatic Acceleration of Organosulfur Redox Behavior by Poly(3,4-Ethylenedioxythiophene). *Electrochem. Solid-State Lett.* **2003**, *6*, A286−A289.
(33) Kiya, Y.; Hatozaki, O.; Oyama, N.; Abruña, H. D. Kinetic Studies for the Electrocatalytic Reduction of Bis(2-Mercapto-1,3,4-Thiadiazoyl)-5,5′-Disulfide at a Poly(3,4-Ethylenedioxythiophene) Film-Modified Electrode via Rotating-Disk Electrode Voltammetry. *J. Phys. Chem. C* **2007**, *111*, 13129−13136.
(34) Lowe, M. A.; Kiya, Y.; Henderson, J. C.; Abruña, H. D. Pendant Thioether Polymer for Redox Capacitor Cathodes. *Electrochem. Commun.* **2011**, *13*, 462−465.
(35) Groenendaal, L.; Jonas, F.; Freitag, D.; Pielartzik, H.; Reynolds, J. R. Poly(3,4-Ethylenedioxythiophene) and Its Derivatives: Past, Present, and Future. *Adv. Mater.* **2000**, *12*, 481−494.
(36) Shin, K.; Obukhov, S.; Chen, J.-T.; Huh, J.; Hwang, Y.; Mok, S.; Dobriyal, P.; Thiyagarajan, P.; Russell, T. P. Enhanced Mobility of Confined Polymers. *Nat. Mater.* **2007**, *6*, 961−965.
(37) Stoller, M. D.; Ruoff, R. S. Best Practice Methods for Determining an Electrode Material's Performance for Ultracapacitors. *Energy Environ. Sci.* **2010**, *3*, 1294−1294.
(38) Feldblyum, J. I.; McCreery, C. H.; Andrews, S. C.; Kurosawa, T.; Santos, E. J. G.; Duong, V.; Fang, L.; Ayzner, A. L.; Bao, Z. Few-Layer, Large-Area, 2D Covalent Organic Framework Semiconductor Thin Films. *Chem. Commun.* **2015**, *51*, 13894−13897.
(39) Lin, S.; Diercks, C. S.; Zhang, Y.-B.; Kornienko, N.; Nichols, E. M.; Zhao, Y.; Paris, A. R.; Kim, D.; Yang, P.; Yaghi, O. M.; et al. Covalent Organic Frameworks Comprising Cobalt Porphyrins for Catalytic CO2 Reduction in Water. *Science* **2015**, *349*, 1208−1213.
(40) Guo, J.; Xu, Y.; Jin, S.; Chen, L.; Kaji, T.; Honsho, Y.; Addicoat, M. A.; Kim, J.; Saeki, A.; Ihee, H.; et al. Conjugated Organic Framework with Three-Dimensionally Ordered Stable Structure and Delocalized π Clouds. *Nat. Commun.* **2013**, *4*, 2736.

DOI: 10.1021/acscentsci.6b00220
ACS Cent. Sci. 2016, 2, 667−673